Desalination and Water Treatment
www.deswater.com
doi: 10.1080/19443994.2013.874705

53 (2015) 3623–3631
March

Taylor & Francis
Taylor & Francis Group

Adsorption kinetics of a cationic dye from wastewater

Özkan Demirbaş*, Mahir Alkan

Faculty of Science and Literature, Department of Chemistry, University of Balikesir, 10145 Balikesir, Turkey
Tel. +90 266 6121000; Fax: +90 266 6121215; email: ozkan@balikesir.edu.tr

Received 2 November 2011; Accepted 26 November 2013

ABSTRACT

The adsorption kinetics and thermodynamics of Maxilon Blue 5G, a cationic textile dye, onto perlite were investigated in aqueous solution in a batch system for determining the effect of contact time, stirring speed, initial dye concentration, initial solution pH, ionic strength and temperature. Experimental data were evaluated according to the pseudo-first, second-order and the Elovich equation, mass transfer and intra-particle diffusion models, and it was found that adsorption kinetics can be described according to the pseudo-second-order model, from which the rate constant and the adsorption capacity were determined. The thermodynamic activation parameters, such as activation energy, enthalpy, entropy and Gibbs free energy, were determined. The obtained results confirmed the applicability of this mineral as an efficient adsorbent for cationic dyes.

Keywords: Kinetics; Thermodynamics; Cationic dye; Perlite; Adsorption

1. Introduction

Various kinds of synthetic dyestuffs appear in the effluents of wastewater in some industries, such as dyestuff, textiles, leather, paper, plastics, etc. [1]. Wastewaters containing dyes are very difficult to treat since the dyes are recalcitrant organic molecules, resistant to aerobic digestion, and are stable to light, heat and oxidizing agents [2]. Such effluents contain a number of contaminants, including acid or caustic, dissolved solids, toxic compounds and colour [3]. Considering both volume-discharged and effluent combustion, the wastewater from the textile industry is rated as the most polluting one among all industrial sectors' wastewaters [4]. Colour is the first contaminant that can be recognized in wastewater. The presence of very small amounts of dyes in water is highly visible and undesirable [5]. Many techniques have been found for the removal of dye-containing wastewater, such as chemical oxidation, membrane filtration, biodegradation, separation and adsorption techniques [6]. The adsorption process is influenced by the nature of the adsorbent and its substituent groups. The presence and the concentration of surface functional groups play an important role in the adsorption capacity and the removal mechanism of the adsorbent [7].

Many workers have been made to find alternative sorbents, particularly for the sorption of basic and acidic dyes, such as activated carbon, unburned carbon [6–9], silica and montmorillonite [10,11], and other adsorbents such as orange peel [12], palm fruit bunch [13], teak wood bark, cotton waste, sugar cane dust [14,15], silica particles [16], chitosan [17], peanut hull [18], pumice powder [19], glass fibres [20], oxihumolite

*Corresponding author.

(oxidized young brown coal) [21] and pyrophyllite [22] have been extensively used as adsorbents.

Perlite is a glassy volcanic rock. The temperature at which its expansion takes place ranges from 1,400 to 2,000°F (760–1,100°C), and a volume increase of 10–20 times is common [23]. Along the Aegean Coast, Turkey possesses about 70% (70×10^9 tons) of the world's known perlite reserves [24]. The uses of expanded perlite (EP) are many and varied and are based primarily upon its physical and chemical properties. Most perlites have high silica content, usually greater than 70%, and are adsorptive [25]. They are chemically inert in many environments, and hence are excellent filter aids and fillers in various processes and materials.

The aim of this study was to determine the adsorption kinetics of cationic dye such as Maxilon Blue 5G (MB-5G) on perlite over a range of physicochemical conditions, which is important to identify various natural environmental systems. A number of experimental parameters in this study are considered, including the effect of stirring speed, initial dye concentration, initial solution pH, ionic strength and solution temperatures. The thermodynamic activation parameters of the process, such as activation energy, enthalpy, entropy and the free energy, were also determined.

2. Materials and methods

2.1. Materials

The EP sample was obtained from Menderes Perlite Processing Plants of Etibank (Izmir, Turkey). The chemical composition of the EP found in Turkey is given in Table 1. The cation exchange capacity (CEC) of the EP was determined by ammonium acetate method and density by the picnometer method [25]. The specific surface area of the EP was measured by BET N_2 adsorption by Micromeritics FlowSorb II-2300 equipment. The results are summarized in Table 2. The sample of EP was subjected to morphological and microstructural analysis using a SCM 5000 Benchtop scanning electron microscope (SEM) (Neoscope).

EP was treated before using in the experiments as follows [25]: the suspension containing 10 g L^{-1} EP was mechanically stirred for 24 h, and after waiting for about 2 min the supernatant suspension was filtered through filter paper. The solid sample was dried at 105°C for 24 h, ground and then sieved by 150 μm sieves. The 150 μm and smaller particles were used in further experiments.

MB-5G [$C_{16}H_{26}N_3O$, M_W: 266 g/mol, λ_{max} = 654 nm] was obtained from Setaş Textile Co. (Bursa, Turkey) [26]. The molecular structure of MB-5G used is shown in Fig. 1. All other chemicals used were of analytical grade. All water used was of MilliQ quality or doubly distilled.

2.2. Experimental procedure

Sorption kinetic experiments were carried out using mechanic stirrer. All of the dye solution was prepared with ultra pure water. Kinetic experiments were carried out by agitating 2 L of dye solution of initial concentration 2×10^{-3} mol/L with dye of EP at a constant agitation speed of 400 rpm, 1×10^{-3} mol/L ionic strength (NaCl), 298 K and pH 8.5. Agitation was done for 60 min, which is more than sufficient time to reach equilibrium at a constant agitation speed of 400 rpm. Preliminary experiments had shown that the effect of the separation time on the adsorbed amount of dye is negligible. The initial tested concentrations of MB-5G solution were 1.5×10^{-3}, 2.0×10^{-3} and 2.5×10^{-3} mol/L. The effect of pH on the amount of colour removal was analysed in the pH range from 5 to 10. The pH was adjusted using 0.1 N NaOH and 0.1 N HCl solutions by using an Orion 920A pH-meter with a combined pH electrode. The pH-meter was standardized with NBS buffers before every measurement. The effect of ionic strength was investigated at 0.001–0.100 mol/L NaCl salt concentrations. The experiments were carried out at 288, 298, 308 and 318 K in a constant temperature bath. Two millilitres

Table 1
Chemical composition of EP

Constituent	Percentage present (%)
SiO_2	72.35
Al_2O_3	12.63
Na_2O	2.82
K_2O	1.51
CaO	1.48
Fe_2O_3	0.98
MgO	0.05
LoI	8.18

Table 2
Some physicochemical properties of EP used this study

Particle size (μm)	−150
Colour	White
pH	7.20
CEC (meq/100 g)	22.50
Density (g ml^{-1})	2.20
Specific suface area (m^2 g^{-1})	7.30

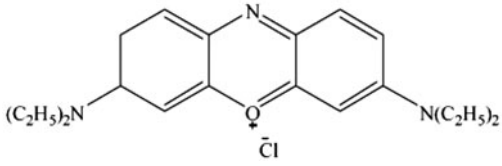

Fig. 1. Structures of MB-5G.

of samples were drawn at suitable time intervals. The samples were then centrifuged for 15 min at 5,000 rpm and the left out concentration in the supernatant solution was analysed using UV–Vis spectrophotometer (Cary 1E UV–Vis spectrophotometer, Varian) by monitoring the absorbance changes at a wavelength of maximum absorbance. Each experimental run continued until no significant change in the dye concentration was measured. Calibration curves were plotted between absorbance and concentration of the dye solution. The adsorbed amount of dye at any time t, q_t, was calculated from the mass balance (Eq. (1)) [26].

$$q_t = (C_0 - C_t)\frac{V}{m} \quad (1)$$

where C_0 and C_t are the initial and liquid-phase concentrations at any time t of dye solution (mol/L), respectively; q_t is the dye concentration on adsorbent at any time t (mol/g), V is the volume of the dye solution (L), and m is the mass of the EP sample used (g) [26].

3. Results and discussion

3.1. Effect of contact and equilibrium times and initial dye concentration

The adsorption of MB-5G dye on EP at different initial concentrations and stirring speed of 400 rpm was studied as a function of contact time in order to determine the equilibrium time. As can be seen clearly in Fig. 2, the perlite and the dye adsorbed on the surface of the perlite show time-dependent morphological changes. Perlite surface morphology completely changed after 60 min. It can be concluded that the images are consistent with experimental data.

Fig. 3 shows the plot of amount of dye adsorbed vs. time at different initial dye concentrations. From the figure, it was observed that the amount of dye adsorbed gets increased from 0.275×10^{-4} to 0.510×10^{-4} mol/g for an increase in initial dye concentration from 1.5×10^{-3} to 2.5×10^{-3} mol/L.

3.2. Effect of stirring speed

The effect of stirring speed on the removal rate of MB-5G with EP was investigated at different stirring speeds, such as 200, 400 and 600 rpm. Fig. 4 shows the sorption of MB-5G by EP adsorbent at different stirring speeds, ranging from 200 to 600 rpm using a contact time of 60 min. The amount of dye adsorbed mass in the sorbent at equilibrium sorption capacity increased with increase in stirring speed. This can be explained by the fact that increasing the agitation speed reduces the film boundary layer surrounding the particles, thus increasing the external film transfer coefficient, and hence the adsorption capacity. This result is surprising since the agitation speed can change the kinetics, not the equilibrium capacity [27]. McKay [28] reported that the rate of dye removal was influenced by the degree of agitation and the uptake increased with stirring rate. The degree of agitation reduced the boundary layer resistance and increased the mobility of the system. An agitation speed of 400 rpm was chosen for further experiments.

3.3. Effect of solution pH

The variation in the removal rate of MB-5G with respect to pH can be elucidated by considering the surface charge of the adsorbent materials. From Fig. 5, it was observed that the solution pH affected the amount of dye adsorbed. The dye uptake was found to increase with increasing pH and it increases from 0.299×10^{-4} to 0.410×10^{-4} mol/g for an increase in pH from 5 to 10. The figure demonstrates that the adsorption increases with increasing pH because of the electrostatic attraction between the dye and the negatively charged EP surface. As the pH increases from 5 to 10, the number of ionisable sites on EP increases. In this case, Eq. (2):

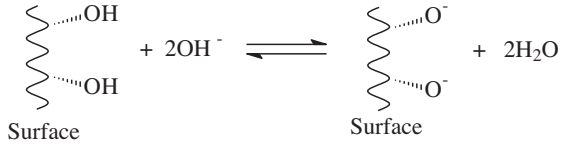

(2)

The removal of dye at higher pH values may be due to the abundance of OH^- ions and because of electrostatic attraction between the negatively charged surface of the adsorbent and the cationic dye molecules [29]. The negatively charged sites favour the adsorption of dye cations due to electrostatic attraction [29]. In this case, it can be written as follows:

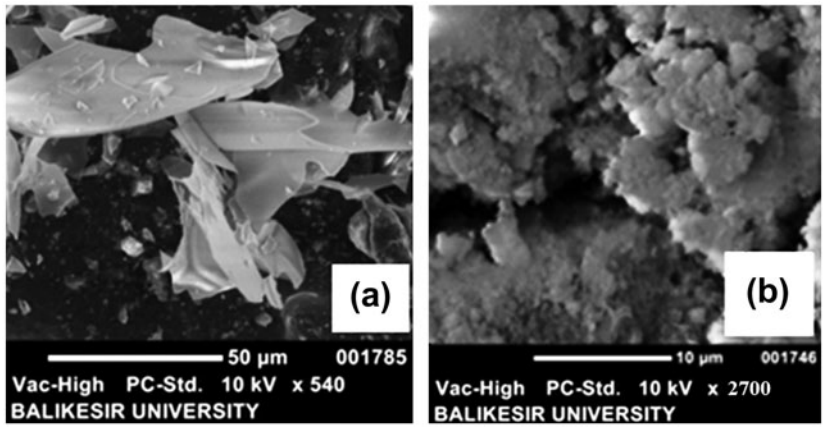

Fig. 2. SEM microphotographs of (a) Expanded perlite and (b) MB-5G adsorbed by expanded perlite after 60 min.

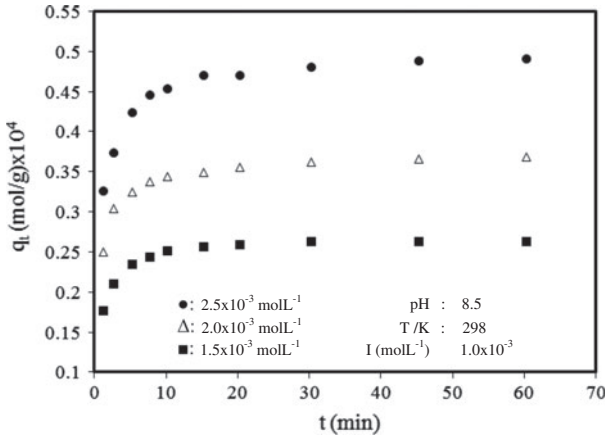

Fig. 3. The effect of initial dye concentration to the adsorption rate of MB-5G on expanded perlite.

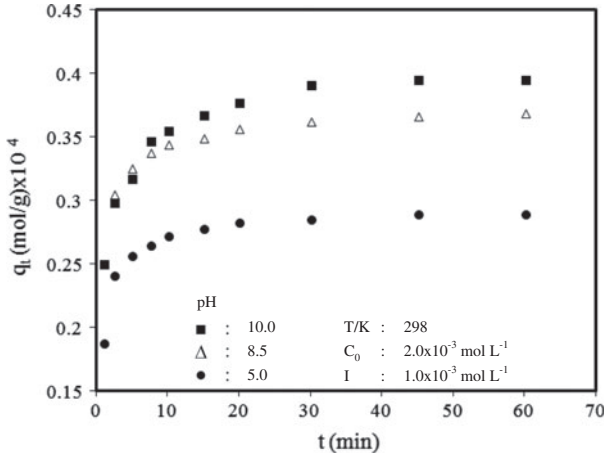

Fig. 5. The effect of solution of pH to the adsorption rate of MB-5G on expanded perlite.

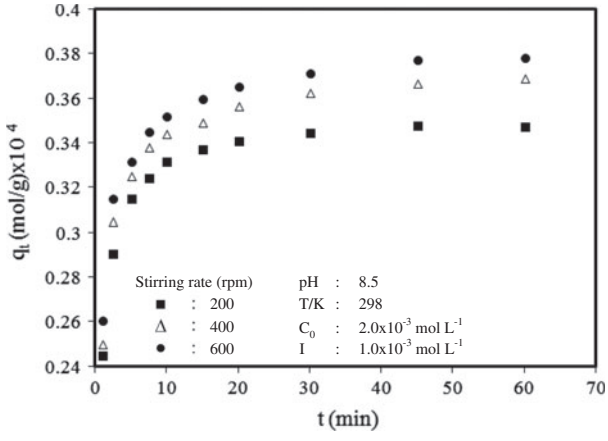

Fig. 4. The effect of stirring speed to the adsorption rate of MB-5G on expanded perlite.

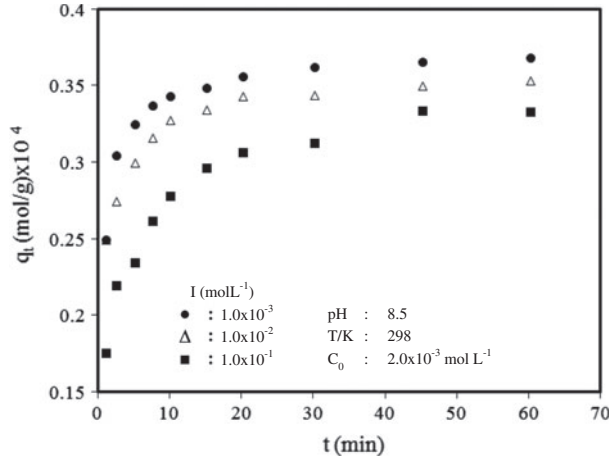

Fig. 6. The effect of ionic strength to the adsorption rate of MB-5G on expanded perlite.

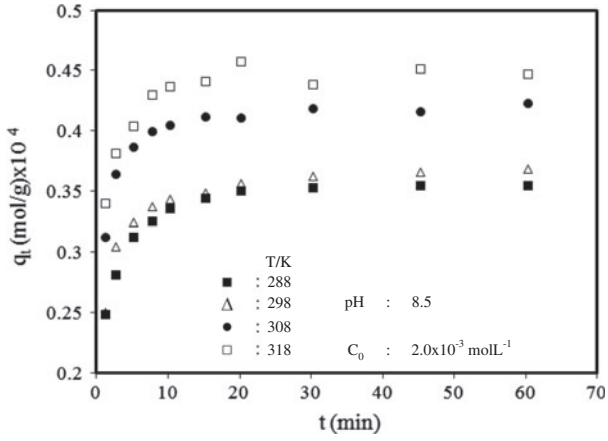

Fig. 7. The effect of temperature to the adsorption rate of MB-5G on expanded perlite.

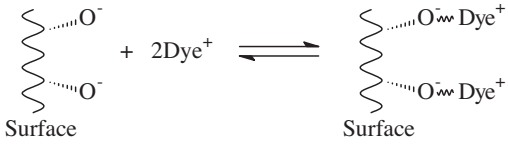

(3)

A similar effect was previously reported by Mall and Upadhyay [30] for methylene blue adsorption on fly ash particles, and Doğan and Alkan [31] for methyl violet adsorption on perlite.

3.4. Effect of ionic strength

The presence of inorganic salt had significantly influenced the adsorption rate of MB-5G. As seen in Fig. 6, the adsorption was found to decrease with increasing ionic strength. Since the salt screens the electrostatic interaction of opposite changes of the oxide surface and the dye molecules, the adsorbed amount will decrease with increase in NaCl concentration [32].

3.5. Effect of temperature

Fig. 7 shows the adsorption kinetics of MB-5G at 288, 298, 308 and 318 K by plotting its uptake capacity, q_t, vs. time at the initial dye concentration of 2×10^{-3} mol/L. Increasing the temperature is known to increase the rate of diffusion of the adsorbate molecules across the external boundary layer and in the internal pores of the adsorbent particle, owing to the decrease in the viscosity of the solution. In addition, changing the temperature will change the equilibrium capacity of the adsorbent for a particular adsorbate [26,32]. When the temperature was raised from 288 to 318 K, the removal of dye by adsorption onto expanded perlite increased from 0.368×10^{-4} to 0.476×10^{-4} mol/g, indicating that the process is endothermic.

3.6. Adsorption kinetics

In order to examine the controlling mechanism of sorption process, several kinetic models were used to

Table 3
Kinetic data calculated for adsorption of MB-5G on expanded perlite

Parameters					Kinetic models								
					Pseudo-first-order	Pseudo-second-order							
T/K	Conc. (mol L^{-1}) × 10^3	pH	Stirring speed (rpm)	[I] (mol L^{-1})	R^2	$q_{e(cal.)}$ (mol g^{-1}) × 10^4	$q_{e(exp.)}$ (mol g^{-1}) × 10^4	k_2 (g mol^{-1} min^{-1})	k_L (L g min^{-1} m^{-2})× 10^3	R^2	h (mol min^{-1} g^{-1}) × 10^4	$t_{1/2}$ (s)	Elovich R^2
298	2	8.5	400	0.001	0.97	0.373	0.368	6212.2	1.806	0.98	5.019	41.00	0.82
308	2	8.5	400	0.001	0.85	0.441	0.440	6942.1	2.872	0.99	7.985	30.74	0.78
318	2	8.5	400	0.001	0.88	0.468	0.476	8302.5	3.899	0.99	11.148	23.78	0.86
298	2	10.0	400	0.001	0.82	0.417	0.410	3171.3	1.186	0.98	3.163	72.23	0.92
298	2	8.5	400	0.001	0.93	0.385	0.382	5081.6	1.614	0.99	4.415	48.28	0.89
298	2	5.0	400	0.001	0.94	0.303	0.299	6934.6	1.367	0.99	3.701	45.12	0.91
298	2	8.5	200	0.001	0.98	0.363	0.360	7319.5	2.064	0.99	5.656	35.56	0.84
298	2	8.5	600	0.001	0.92	0.395	0.391	4910.5	1.647	0.98	4.492	48.69	0.83
298	1.5	8.5	400	0.001	0.88	0.277	0.275	9141.4	2.010	0,98	4.080	37.47	0.90
298	2.5	8.5	400	0.001	0.91	0.515	0.510	3322.4	1.510	0.99	5.130	55.43	0.88
298	2	8.5	400	0.010	0.92	0.371	0.367	4601.0	1.356	0.99	3.679	55.57	0.97
298	2	8.5	400	0.100	0.94	0.355	0.346	2105.0	0.571	0.99	1.504	128.75	0.96

test the experimental data. From a system design viewpoint, a lumped analysis of sorption rates is thus sufficient for practical operation.

3.6.1. Pseudo first-order equation

The pseudo first-order equation is generally expressed as follows [33]:

$$\ln(q_e - q_t) = \ln q_e - k_1 t \quad (4)$$

where q_e and q_t are the amount of dye ions adsorbed at equilibrium at time t (mol g^{-1}), respectively, and k_1 is the rate constant of pseudo-first-order adsorption (min^{-1}). The fitting results are given in Table 3.

3.6.2. Pseudo-second-order equation

If the rate of adsorption is a second-order mechanism, the pseudo-second-order equation is expressed by Eq. (5) [33]:

$$\frac{t}{q_t} = \frac{1}{k_2 q_e^2} + \frac{1}{q_e} t \quad (5)$$

where q_e is the amount of dye ions adsorbed at equilibrium (mol g^{-1}) and k_2 is the equilibrium rate constant of pseudo-second-order sorption (g (mol min)$^{-1}$).

The half-adsorption time of the dye ions, $t_{1/2}$, is expressed by Eq. (6):

$$t_{1/2} = \frac{1}{k_2 q_e} \quad (6)$$

The initial adsorption rate, h (mol/(g min)), is expressed by Eq. (7):

$$h = k_2 q_e \quad (7)$$

The values k_2, q_e, $t_{1/2}$ and h are given in Table 3. As shown in Table 3, experimental data can be explained by pseudo-second-order kinetic equations.

3.6.3. Elovich equation

In reactions involving chemisorption of adsorbates on a solid surface without desorption of the products, the rate decreases with time due to an increased surface coverage. One of the most useful models for describing such activated adsorption is the Elovich Eq. (8) [34,35]:

$$q_t = \beta \in (\alpha\beta) + \beta \in t \quad (8)$$

where α is the initial adsorption rate (mol/(g min)) and β is related to the extent of surface coverage and activation energy for chemisorption (g/mol). The testing of experimental data for correspondence with the Elovich equation carried out by plotting q_t vs. $\ln t$ and correlation coefficients are shown in Table 3. As

Table 4
Adsorption mechanism and diffusion coefficients of MB-5G on expanded perlite

	Mechanism of adsorption									
	Mass transfer	Intra-particle diffusion								
Parameters T/K	Conc. (mol L^{-1}) × 10^3	pH	Stirring Speed (rpm)	[I] (mol L^{-1})	R^2	$k_{int,1}$ × 10^5 mol g^{-1} $min^{-1/2}$	R_1^2	$k_{int,2}$ × 10^6 mol g^{-1} $min^{-1/2}$	R_2^2	D (cm^2 s^{-1}) × 10^9
288	2	8.5	400	0.001	0.58	3.91	0.96	2.94	0.72	5.51
308	2	8.5	400	0.001	0.80	4.27	0.90	3.89	0.82	7.35
318	2	8.5	400	0.001	0.90	4.36	0.96	3.97	0.91	9.50
298	2	10	400	0.001	0.71	4.58	0.94	7.00	0.84	3.13
298	2	8.5	400	0.001	0.79	4.25	0.88	4.36	0.91	4.68
298	2	5.0	400	0.001	0.97	3.67	0.84	2.90	0.86	5.01
298	2	8.5	200	0.001	0.82	3.95	0.90	2.68	0.84	6.35
298	2	8.5	600	0.001	0.68	4.05	0.87	4.55	0.91	4.64
298	1.5	8.5	400	0.001	0.63	3.44	0.93	1.81	0.76	6.03
298	2.5	8.5	400	0.001	0.67	6.15	0.97	6.02	0.89	4.08
298	2	8.5	400	0.010	0.88	3.35	0.98	4.26	0.89	4.06
298	2	8.5	400	0.100	0.68	4.05	0.93	9.44	0.90	1.75

shown in Table 3, Elovich equation is not compatible with the experimental data.

3.6.4. The diffusion coefficients, intra-particle diffusion equation and mass transfer

The fractional approach to equilibrium changes according to the function of $(D_t/r^2)^{1/2}$, where r is the particle radius and D the diffusivity of solute within the particle. The diffusion coefficient largely depends on the surface properties of adsorbents. The diffusion coefficients for the adsorption of MB-5G on expanded perlite particles have been calculated under various conditions by employing the following Eq. (9):

$$t_{1/2} = \frac{0.030 r_0^2}{D} \tag{9}$$

where D is the diffusion coefficient with the unit cm^2/s; $t_{1/2}$ is the time (s) for half adsorption; and r_0 is the radius of the adsorbent particle in cm. The value of r_0 was calculated as 2.5×10^{-3} cm for expanded perlite sample. In these calculations, it has been assumed that the solid phase consists of spherical particles with an average radius between the radii corresponding to upper- and lower-size fractions. Table 4 has shown the diffusion coefficients calculated for adsorption of MB-5G on expanded perlite from aqueous solutions. We found that the diffusion coefficients in this study changed in the range of $1.75–9.50 \times 10^{-9}$ cm^2/s under various conditions.

The initial rate of the intraparticle diffusion is calculated by the following Eq. (10) [29]:

$$q_t = k_{int} t^{1/2} + C \tag{10}$$

where k_{int} is the intraparticle diffusion rate constant (mg $(g\,min^{1/2})^{-1}$ and is given in Table 4.

The intraparticle diffusion coefficient for the sorption of MB-5G was calculated from the slope of the plot of square root of time ($min^{0.5}$) vs. amount of dye adsorbed (mol/g). Previous studies by various researchers showed that the plot between q_t and $t^{0.5}$ represents multi-linearity, which characterizes the two or more steps involved in sorption process [29,31]. Fig. 8 shows the plot between q_t and $t^{0.5}$ for MB-5G onto expanded perlite particles. From Fig. 8 (other figures not shown), it can be seen that the sorption process tends to be followed by two phases. It was found that the initial linear portion ended with a smooth curve followed by second linear portion. The two phases in the intraparticle diffusion plot suggest that the sorption process proceeds by first surface sorption, and then intraparticle diffusion. The initial curved portion of the plot indicates boundary layer effect while the second linear portion is due to intraparticle or pore diffusion. The calculated intraparticle diffusion coefficient values, $k_{int,1}$ and $k_{int,2}$, at different conditions are shown in Table 4. Since $k_{int,1}$ values for the first part of the plot are high, this step is not a rate-limiting step. The slope of the second linear portion of the plot has been defined as the intraparticle diffusion parameter $k_{int,2}$ (mol/(g $min^{0.5}$)) [36].

For mass transfer, a linear graphical relation between $\ln[(C_t/C_0)-1/(1+mK)]$ vs. t was not obtained (equation from M. Doğan et al. et al. [29]). This result indicates that the model mentioned above for the system is not valid. The values of regression coefficient calculated from the equation mentioned above are given in Table 4.

3.7. Thermodynamic parameters

The second-order rate constants are used to estimate the activation energy of the MB-5G adsorption on expanded perlite using Arrhenius Eq. (11):

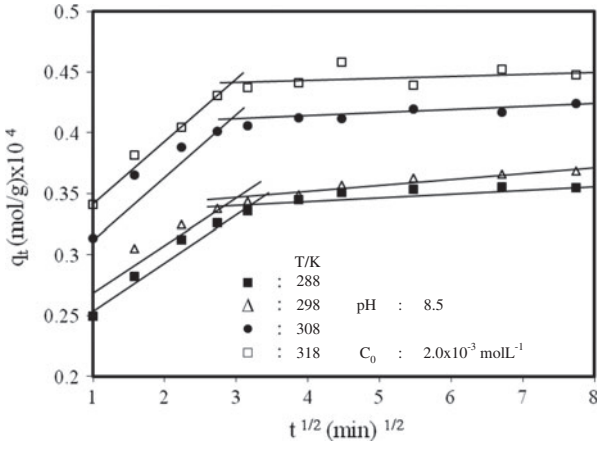

Fig. 8. Intra-particle diffusion plots for different temperatures.

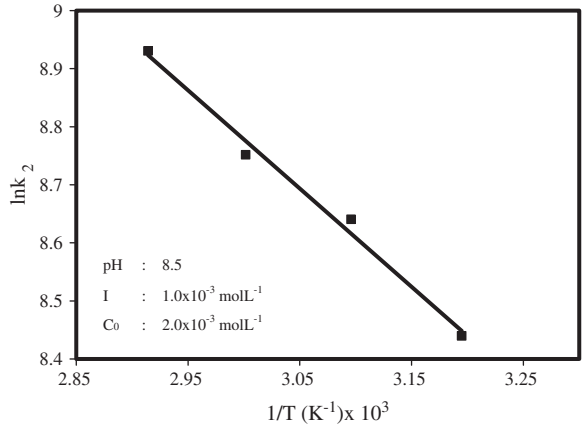

Fig. 9. Arrhenius plot for the adsorption of MB-5G on expanded perlite.

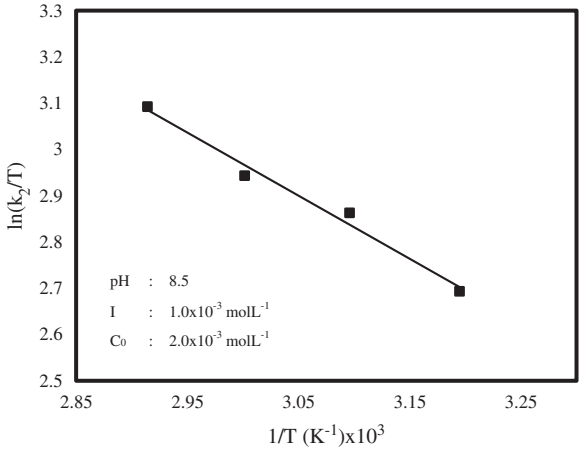

Fig. 10. Plot of ln (k_2/T) vs. $1/T$ for adsorption of MB-5G on expanded perlite.

$$\ln k_2 = \ln A - \frac{E_a}{R_g T} \tag{11}$$

where E_a is the activation energy (J/mol), k_2 is the rate constant of sorption (g/(mol s)), A is the Arrhenius factor, which is the temperature-independent factor (g/(mol s)), R_g is the gas constant (J/(K mol)) and T is the solution temperature (K). The slope of the plot of ln k_2 vs. $1/T$ is used to evaluate E_a, which was found to be 22.44 kJ/mol physisorption (Fig. 9). Low activation energies (5–40 kJ/mol) are characteristics for physisorption, while higher activation energies (40–800 kJ/mol) suggest chemisorption [26,29]. Therefore, the thermodynamic activation parameters of the process, such as enthalpy ΔH^*, entropy ΔS^* and free energy ΔG^*, were determined using the Eyring Eq. (12) [37]:

$$\ln\left(\frac{k_2}{T}\right) = \ln\left(\frac{k_b}{h}\right) + \frac{\Delta S^*}{R_g} - \frac{\Delta H^*}{R_g T} \tag{12}$$

where k_b is the Boltzmann constant (1.3807×10^{-23} J/K), h is the Planck constant (6.6261×10^{-34} J s) and R_g is the ideal gas constant (8.314 J mol^{-1} K^{-1}. Fig. 10 shows the plot of ln (k_2/T) against $1/T$. The result obtained for the change of Gibbs energy are + 58.23 kJ/mol at 298 K. This indicated that the adsorption reaction was not a spontaneous one and that the system gained energy from an external source. The value of the standard enthalpy change (18.25 kJ/mol) indicates that the adsorption is physical in nature involving weak forces of attraction and is also endothermic. At the same time, the low value of ΔH^* implies that there was loose bonding between the adsorbate molecules and the adsorbent surface [38]. The negative standard entropy change (ΔS^*) value (−165.4 J/(K mol)) corresponds to a decrease in the degree of freedom of the adsorbed species.

4. Conclusions

The present study shows that expanded perlite can be used as an adsorbent for the removal of MB-5G from its aqueous solutions. The amount of dye uptake (mol/g) was found to increase with increase in contact time, initial dye concentration, stirring speed, pH and solution temperature, and found to decrease with increase in ionic strength. The adsorption system studied belongs to the second-order kinetic model. The dye uptake process was found to be controlled by intraparticle diffusion. Thermodynamic activation parameter shows that the process is endothermic. The positive value of the Gibbs energy change of the adsorption indicates that the adsorption is not spontaneous. The positive value of the enthalpy change of the adsorption shows that the adsorption is an endothermic process. Thus, raising the temperature leads to higher MB-5G adsorption at equilibrium. The kinetic data may be useful for environmental technologists in designing treatment plants for colour removal from wastewaters enriched with MB-5G. Expanded perlite has a high potential to adsorb these dyes from aqueous solutions. Therefore, it can be effectively used as an adsorbent for the removal of this dye from wastewaters.

References

[1] M.-S. Chiou, P.-Y. Ho, H.-Y. Li, Adsorption of anionic dyes in acid solutions using chemically cross-linked chitosan beads, Dyes Pigm. 60 (2004) 69–84.
[2] G. Crini, Non-conventional low-cost adsorbents for dye removal: A review, Bioresour. Technol. 97 (2006) 1061–1085.
[3] J. Yener, T. Kopac, G. Dogu, T. Dogu, Adsorption of Basic Yellow 28 from aqueous solutions with clinoptilolite and amberlite, J. Colloid Interf. Sci. 294 (2006) 255–264.
[4] K.P. Singh, D. Mohan, S. Sinha, G.S. Tondon, D. Gosh, Color removal from wastewater using low-cost activated carbon derived from agricultural waste material, Ind. Eng. Chem. Res. 42 (2003) 1965–1976.
[5] I.M. Banat, P. Nigam, D. Singh, R. Marchant, Microbial decolorization of textile-dyecontaining effluents: A review, Bioresour. Technol. 58 (1996) 217–227.
[6] K.K.H. Choy, G. McKay, J.F. Porter, Sorption of acid dyes from effluents using activated carbon, Resour. Conserv. Recycl. 27 (1999) 57–71.
[7] K.S. Yenisoy, A. Aygun, M. Gunes, E. Tahtasakal, Physical and chemical characteristics of polymer-based spherical activated carbon and its ability to adsorb organics, Carbon 42 (2004) 477–484.

[8] M. Basibuyuk, C.F. Forster, An examination of the adsorption characteristics of a basic dye (Maxilon Red BL-N) on to live activated sludge system, Process Biochem. 38 (2003) 1311–1316.
[9] S. Wang, H. Li, Dye adsorption on unburned carbon: Kinetics and equilibrium, J. Hazard Mater. 126(1–3) (2005) 71–77.
[10] G. McKay, M.S. Otterburn, A.G. Sweeney, Removal of colour from effluent using various adsorbents–III. Silica: Rate processes, Water Res. 14 (1980) 15–20.
[11] C.-C. Wang, L.-C. Juang, T.-C. Hsu, C.-K. Lee, J.-F. Lee, F.-C. Huang, Adsorption of basic dyes onto montmorillonite, J. Colloid Interface Sci. 273 (2004) 80–86.
[12] C. Namasivayam, N. Muniasamy, K. Gayatri, M. Rani, K. Ranganathan, Removal of dyes from aqueous solutions by cellulosic waste orange peel, Bioresour. Technol. 57(1) (1996) 37–43.
[13] Y.S. Ho, G. Mckay, Sorption of dye from aqueous solution by peat, Chem. Eng. J. 70(2) (1998) 115–124.
[14] G. McKay, J.F. Porter, G.R. Prasad, The removal of dye colour from aqueous solutions by adsorption on low-cost materials, Water, Air, Soil Pollut. 114(3/4) (1999) 423–438.
[15] S.D. Khattri, M.K. Singh, Colour removal from dye wastewater using sugar cane dust as an adsorbent, Adsorp. Sci. Technol. 17(4) (1999) 269–282.
[16] T. Jesionowski, Characterisation of pigments obtained by adsorption of C.I. Basic Blue 9 and C.I. Acid Orange 52 dyes onto silica particles precipitated via the emulsion route, Dyes Pigm. 67 (2005) 81–92.
[17] W.S. Wan Ngah, L.C. Teong, M.A.K.M. Hanafiah, Adsorption of dyes and heavy metal ions by chitosan composites: A review, Carbohyd. Polym. 83 (2011) 1446–1456.
[18] G. Renmin, S. Yingzhi, C. Jian, L. Huijun, Y. Chao, Effect of chemical modification on dye adsorption capacity of peanut hull, Dyes Pigm. 67 (2005) 175–181.
[19] A. Feryal, Adsorption of basic dyes from aqueous solution onto pumice powder, J. Colloid Interface Sci. 286 (2005) 455–458.
[20] C. Sampa, K.D. Binay, On the adsorption and diffusion of methylene blue in glass fibers, J. Colloid Interface Sci. 286 (2005) 807–811.
[21] J. Pavel, S. Pavel, M.R. Sylvie, Sorption of basic and acid dyes from aqueous solutions onto oxihumolite, Chemosphere 59 (2005) 881–886.
[22] G. Aslıhan, S. Savas, B. Sedat, M.M. Ali, Adsorption and kinetic studies of cationic and anionic dyes on pyrophyllite from aqueous solutions, J. Colloid Interface Sci. 286 (2005) 53–60.
[23] P.W. Harben, R.L. Bates, Industrial Minerals Geology and World Deposits, Metal Bulletin, London, 1990.
[24] S.S. Uluatam, Assessing perlite as a sand substitute in filtration, J. AWWA. 70 (1991) 70–71.
[25] Ö Demirbaş, M. Alkan, M. Doğan, The removal of victoria blue from aqueous solution by adsorption on a low-cost material, Adsorption 8 (2002) 341–349.
[26] M. Alkan, M. Doğan, Y. Turhan, Ö. Demirbaş, P. Turan, Adsorption kinetics and mechanism of maxilon Blue 5G dye on sepiolite from aqueous solutions, Chem. Eng. J. 139 (2008) 213–223.
[27] G. Crini, H.N. Peindy, F. Gimbert, C. Robert, Removal of C.I. Basic Green 4 (Malachite green) from aqueous solutions by adsorption using cyclodextrin-based adsorbent, Separ. Purif. Technol. 53 (2007) 97–110.
[28] G. McKay, Adsorption of dyestuffs from aqueous solutions with activated carbon I: Equilibrium and batch contact-time studies, J. Chem. Technol. Biotechnol. 32 (1982) 759.
[29] M. Doğan, M. Alkan, Ö. Demirbaş, Y. Özdemir, C. Özmetin, Adsorption kinetics of Maxilon Blue GRL onto sepiolite from aqueous solutions, Chem. Eng. J. 124 (2006) 89–101.
[30] I.D. Mall, S.N. Upadhyay, Treatment of methyl violet bearing wastewater from paper mill effluent using low cost adsorbents, J. Indian Pulp Paper Technol. Assoc. 7(1) (1995) 51–57.
[31] M. Doğan, M. Alkan, Adsorption kinetics of methyl violet onto perlite, Chemosphere 50 (2003) 517–528.
[32] N. Tekin, O Demirbaş, M. Alkan, Adsorption of cationic polyacrylamide onto kaolinite, Micropor. Mesopor. Mater 85(3) (2005) 340–350.
[33] Y.S. Ho, G. McKay, Pseudo-second order model for sorption processes, Process Biochem. 34 (1999) 451–465.
[34] K. Klusácek, R.R. Hudgins, P.L. Silveston, Multiple steady states of an isothermal catalytic reaction with Elovich adsorption, Chem. Eng. Sci. 44 (1989) 2377–2381.
[35] C. Aharoni, S. Sideman, E. Hoffer, Adsorption of phosphate ions by colloid ion-coated alumina, Chem. Technol. Biotechnol. 29 (1979) 404–412.
[36] N. Kannan, M. Sundaram, Kinetics and mechanism of removal of methylene blue by adsorption on various carbons—a comparative study, Dyes Pigm. 51 (2001) 25–40.
[37] K.J. Laidler, J.M. Meiser, Physical Chemistry, Houghton Mifflin, New York, NY, 1999, p. 852.
[38] D. Singh, Studies of the adsorption thermodynamics of oxamyl on fly ash, Adsorpt. Sci. Technol. 18(8) (2000) 741–748.